A multi-scale magnetotail reconnection event at Saturn and associated flows: Cassini/UVIS observations

A.Radioti[a], D. Grodent[a], X. Jia[b], J.-C. Gérard[a], B. Bonfond[a], W. Pryor[c], J. Gustin[a], D. Mitchell[d], C.M. Jackman[e]

[a]*Laboratoire de Physique Atmosphérique et Planétaire (LPAP), Université de Liège, Liège, Belgium.*
[b]*Department of Atmospheric, Oceanic, and Space Sciences, University of Michigan, USA*
[c]*Science Department, Central Arizona College, Coolidge, Arizona, USA*
[d]*Applied Physics Laboratory, Johns Hopkins University, Laurel, Maryland, USA*
[e]*School of Physics and Astronomy, University of Southampton, Southampton, England*

Abstract

We present high-resolution Cassini/UVIS (Ultraviolet Imaging Spectrograph) observations of Saturn's aurora during May 2013 (DOY 140-141). The observations reveal an enhanced auroral activity in the midnight-dawn quadrant in an extended local time sector (∼02 to 05 LT), which rotates with an average velocity of ∼ 45% of rigid corotation. The auroral dawn enhancement reported here, given its observed location and brightness, is most probably due to hot tenuous plasma carried inward in fast moving flux tubes returning from a tail reconnection site to the dayside. These flux tubes could generate intense field-aligned currents that would cause aurora to brighten. However, the origin of tail reconnection (solar wind or internally driven) is uncertain. Based mainly on the flux variations, which do not demonstrate flux closure, we suggest that the most plausible scenario is that of internally driven tail reconnection which operates on closed field lines. The observations also reveal multiple intensifications within the enhanced region suggesting an x-line in the tail, which extends from 02 to 05 LT. The localised enhancements evolve in arc and spot-like small scale features, which resemble vortices mainly in the beginning of the sequence. These auroral features could be related to plasma flows enhanced from reconnection which diverge into multiple narrow channels then spread azimuthally and radially. We suggest that the evolution of tail reconnection at Saturn may be pictured by an ensemble of numerous narrow current wedges or that inward transport initiated in the reconnection region could be explained by multiple localised flow burst events.

The formation of vortical-like structures could then be related to field-aligned currents, building up in vortical flows in the tail. An alternative, but less plausible, scenario could be that the small scale auroral structures are related to viscous interactions involving small-scale reconnection.

Keywords:

1. Introduction

Saturn's magnetotail is suggested (i.e. Cowley et al. (2005); Jackman et al. (2011)) to be influenced by a combination of solar wind (Dungey, 1961) and internally driven (Vasyliūnas, 1983) magnetic reconnection. In the Dungey cycle, reconnected open flux tubes are transported over the poles by the solar wind, before reconnecting in the tail. The newly closed field lines in the tail are then expected to convect around the flanks back to the dayside. The Vasyliūnas cycle is an internally driven process, in which the planet's rapid rotation combined with the mass-loading of flux tubes fed by internal plasma sources (Enceladus and its neutral cloud) lead to reconnection on closed field lines. The closed field lines are then accelerated back to the dayside via the dawn flank. Theoretical studies (Cowley et al., 2005; Badman and Cowley, 2007) and recent global MHD simulations of Saturn's magnetosphere (Jia et al., 2012) suggest that Dungey-type reconnection typically results in hotter and more depleted flux tubes with faster bulk flows from the reconnection site compared to those produced directly by the Vasyliūnas-cycle reconnection, mainly due to the different plasma and field conditions of the inflow region surrounding the reconnection site. When only the Vasyliūnas-cycle is operating, such as during intervals of southward IMF, the associated X-line is suggested to form primarily in the midnight to dawn sector. When both processes are at work, the pure Vasyliūnas-cycle X-line is confined to a limited region in the pre-midnight sector while the Dungey-cycle X-line, albeit variable both in space and time, is suggested primarily in the midnight-to-dawn sector, adjacent to the Vasyliūnas-cycle X-line. Additionally, another process which is suggested to influence Saturn's magnetotail is the viscous interaction of the solar wind with the planetary magnetosphere, which involves magnetic reconnection on a small scale (Delamere and Bagenal, 2013). The authors propose that mass loading and related viscous boundary processes contribute to the magnetotail structure.

The quasi-continuous main auroral emission at Saturn is suggested to be produced by magnetosphere-solar wind interaction, through the shear in rotational flow across the open closed field line boundary (OCFLB) (e.g. Bunce et al. (2008)). Expansion or contraction of the polar cap size, in response to magnetic reconnection, gives evidence on the mechanisms which couple solar wind mass, energy and momentum into the magnetosphere of Saturn (Badman et al., 2005; Radioti et al., 2011; Badman et al., 2014). Low-latitude magnetopause reconnection, which occurs for northward IMF at Saturn, creates new open flux and increases the polar cap size (Cowley et al., 2005; Badman et al., 2005; Jackman and Cowley, 2006; Radioti et al., 2011). Tail reconnection in the Dungey-cycle manner is expected to result in bright and fast rotating aurorae, which expand poleward in the dawn sector, reducing significantly the size of the polar cap and thus resulting in closure of flux (Cowley et al., 2005; Badman et al., 2005; Jia et al., 2012). Finally, tail reconnection on closed field lines (Vasyliūnas-type) is not expected to modify the polar cap size as it does not change the total amount of flux.

UV intensification of Saturn's dawn auroras, together with simultaneous enhancement of ENA emission and Saturn kilometric radiation (SKR) demonstrated the initiation of several recurrent acceleration events in the midnight to dawn quadrant at radial distances of 15-20 R_S (Mitchell et al., 2009). The authors associated these injection events with reconnection in the tail. Approximately 45 min earlier, localised small scale intensifications, located poleward of the main nightside auroral emission, are suggested to be signatures of dipolarizations in the tail (Jackman et al., 2013). The authors suggested that diversion of cross-tail current leads to discrete auroral spots, similar to the terrestrial 'substorm current wedge' paradigm (McPherron et al., 1973). The small scale intensifications are believed to be precursors to a more intense activity following tail reconnection (Mitchell et al., 2009). A similar event of intense auroral activity in the dawn auroral sector was recently observed by the Ultraviolet Imaging Spectrograph (UVIS) instrument on board Cassini. It was characterised by significant flux closure with a rate ranging from 200 to 1000 kV (Radioti et al., 2014). Additionally, Nichols et al. (2014) presented Hubble Space Telescope observations taken in April 2013 (D0Y 95: 1740 to 1818 UT), which revealed auroral intensifications in the dawn auroral sector, propagating at $\sim 330\%$ rigid corotation from near ~ 01 h LT toward 08 h LT. The authors suggested that these emissions are indicative of ongoing, bursty reconnection of lobe flux in the magnetotail, with flux closure rates of 280 kV. In the same study the authors reported on another similar although less pronounced event which operated between

1727 and 1910 UT and on the beginning of a third one between 2053 to 2121 UT. Here we present an auroral intensification at Saturn's dawn sector captured by Cassini/UVIS in May 2013 (DOY 140 1942 UT to DOY 141 0100 UT), the very beginning of which has also been observed by Hubble Space Telescope (HST) in the aforementioned study.

2. Auroral dawn enhancement

2.1. UVIS observations on DOY 140-141, 2013

Figure 1 shows a sequence of polar projections of Saturn's northern aurora obtained with the FUV channel (111-191 nm) of the UVIS instrument (Esposito et al., 2004) onboard Cassini on DOY 140-141, 2013. The projections are constructed by combining slit scans, which provide 64 spatial pixels of 1 mrad (along the slit) by 1.5 mrad (across the slit), using the method described by Grodent et al. (2011). Each auroral image, except for the third one (2149 UT - single image), is constructed by adding two subimages showing complementary portions of the auroral region taken ~30 min apart. The displayed time corresponds to the starting time of the first subimage. During the start of the 1st image and the end of the last image the sub-spacecraft planetocentric latitude increased from 23 to 48 degrees and the spacecraft altitude changed from 5.2 to 5.9 R_S. Because of the relatively high sub-spacecraft latitude, the limb brightening effect is limited and therefore no correction was applied.

The auroral emissions reveal an intensification on the main emission (included in the red rectangle) which starts in the midnight-dawn quadrant. In the first images, it extends from ~02 to 05 LT and propagates with time around to 10 LT. This auroral region displays features with a large range of brightness. Localised peaks could be as bright as 30 kR and others could reach values in excess of 300 kR. We determine the velocity of the enhanced auroral feature by tracking the motion of its barycenter. We observe it to rotate with the planet at 56% of rigid corotation at the beginning of the sequence, while its velocity drops to ~27% of rigid corotation at the end. We consider an error bar of ±5% of rigid corotation which corresponds to an uncertainty of 2° (1 pixel) in selecting the border of the enhancement. The mean value of the velocity along the sequence is ∼ 45% of rigid corotation. The morphology of the feature is consistent with the auroral signatures of bursts of tail reconnection discussed in earlier theoretical and observational studies (Cowley et al., 2005; Mitchell et al., 2009; Clarke et al., 2009; Jia et al., 2012; Nichols et al., 2014; Radioti et al., 2014). The major auroral dawn enhancement discussed here is quite bright in several images at the local time location of Mimas, which changes from 3 to 9 local time during this interval. Saturn's auroral enhancements on the main auroral emission are observed to be associated with the local time location of Mimas (and sometimes of Enceladus) (Pryor (2012); Mitchell et al. (2014b)).

In the same sequence, a high latitude ($\sim$80°) feature is observed between 06 and 10 LT, located poleward of the main emission and it is indicated by the yellow arrow. It gradually moves to lower latitudes ($\sim$78°) and tends to vanish with time. It subcorotates at $\sim$30% of rigid corotation at the beginning of the sequence, then its velocity gradually reduces and the feature remains stagnant towards the end of the sequence. This feature could be possibly related to high-latitude reconnection under southward IMF conditions (Gérard et al., 2005; Bunce et al., 2004) and thus it would be on open field lines. Another possibility is that this feature is related to the excess flux of the bursty reconnection of lobe flux in the magnetotail, whose auroral signature is observed by HST between 1727 and 1910 UT (Nichols et al., 2014). This high-latitude feature is observed until the end of the HST sequence at 2121 UT.

The main emission oval is slightly shifted a couple of degrees during the whole interval namely the afternoon sector shifts to lower latitudes while the pre-dawn region shifts poleward. Previous studies (Nichols et al., 2010) showed that the centers of the auroral ovals at Saturn have been observed to oscillate along an ellipse with a latitudinal amplitude of 1-2° due to an external magnetospheric current system. We estimated the direction of the maximum equatorward displacement of the northern hemisphere for our observed interval, based on the azimuthal direction of the effective dipole and according to the method described in Badman et al. (2012). The azimuthal directions of the effective dipoles are taken from the empirical model by Provan et al. (2013). We find that the maximum equatorward displacement of the main emission is directed towards $\sim$ 0.6 LT during the time the second image was taken (start time 2046 UT) while it is directed towards $\sim$ 11 LT when the last image was taken (start time 0100 UT). The direction of the displacement is consistent with our observations.

We estimate the flux variations during the observed auroral sequence. For the estimation of the amount of open flux contained within the polar cap region we use a flux function, described in detail in Radioti et al. (2011). The polar cap boundaries are estimated automatically based on the cut-off intensity (4 kR), which corresponds to an average value of the day and night glow emission of this dataset. In our flux estimation we do not include the first image as the UVIS observational geometry provided an incomplete view of the auroral region. For the same reason the local time section between 21 and 02 LT in the auroral image taken at 2149 UT is not covered. For this image the calculation of the polar cap boundary at this local time sector is based on the average boundaries from the previous (2046 UT) and next (2253 UT) observations.

An example of the selected regions, used to calculate the flux is shown in panel b of Figure 2. The boundaries of all regions of interest are indicated by different symbols. The flux variation of the high latitude emission pointed out by the yellow arrow in Figure 1, whose origin is uncertain (open flux due to high latitude reconnection (Gérard et al., 2005) or excess of closed flux of the bursty reconnection of lobe flux Nichols et al. (2014)) is shown with the orange asterisks in panel a of Figure 2. This flux is observed to decrease with time. We also calculate the total open flux at a given time using two methods. In the first, we calculate the total open flux assuming that the high latitude feature is related to closed flux (excess of closed flux due to tail reconnection) and denote this quantity as 'flux 1'. The 'flux 1' variations as a function of time as well as the boundaries of this region are shown with the blue diamonds in Figure 2 panel a and b, respectively. The open flux 1 values are varying between 20 and 25.5 GWb, which is consistent with the average open flux range (10-50 GWb) estimated based on a large set of HST images (Badman et al., 2014). 'Flux 1' is shown to increase with time from ~ 20 to 25.5 GWb within ~ 4 hours, indicative of opening of flux with a reconnection rate of ~ 360 kV (1 kV = 10^{-6} GWb s^{-1}). This rate lies in the extreme upper average reconnection rate range estimated by Badman et al. (2014) and is suggestive of a large dayside reconnection event. Also according to Jackman et al. (2004), which derived dayside reconnection rates from an empirical formula adapted from Earth, 360 kV would correspond to a strong solar wind compression. It should be noted that there is no clear auroral evidence of low latitude dayside reconnection during this observed interval, which could have justified opening of flux. Auroral signatures of dayside reconnection are described as bifurcations of the main emission, namely auroral arcs with one arc attached to the main emission and the other one bending into the polar cap, which are observed in the post-noon local time sector (i.e. as described in Radioti et al. (2011)). These auroral reconnection signatures are accompanied by reconnection voltages of 280 kV. The absence of such features makes the scenario of the total flux to be described by the quantity 'flux 1' less valid. In the second method, we calculate the total open flux assuming that the high latitude feature is on open field lines (high latitude reconnection), and denote this quantity as 'flux 2'. In that case the boundary used to estimate the open 'flux 2' is drawn on the auroral emission in panel b by the red line. 'Flux 2' remains almost constant with time (red line Figure 2 panel a), while in the second part of the sequence it slightly increases (6%). The open flux 2 values are varying between 26 and 28 GWb, which is within the average open flux range (Badman et al., 2014).

The polar cap boundaries are estimated based on 4 kR cut-off intensity, which corresponds to the average value of the day and night glow emission of this dataset, as explained above. In order to test the significance of this threshold on the flux variations, we also estimate the flux for different thresholds: 3 and 5 kR (red dashed lines for 'flux 2'). It is demonstrated that while the net amount of open 'flux 2' changes depending on the chosen threshold, the open flux variation as a function of time has a similar trend whatever the initial threshold. We also drew error bars on the 'flux 2', which are estimated by randomly varying the auroral detection threshold from 3 to 5 kR for each local time. This variation range corresponds to Poisson error related to the number of counts included in our initial chosen threshold of 4 kR. The small variations of the 'flux 2' as a function of time are within the error bar.

2.2. On the origin of the auroral enhancement

The auroral brightening in the dawn region can be due to hot tenuous plasma carried inward in fast moving flux tubes returning from tail reconnection site to the dayside. Such flux tubes may generate intense field-aligned currents that would cause aurora to brighten. Judging only from the expansion of the dawn auroral emission poleward, during the first hour of the sequence, one could argue that the auroral enhancement is evidence of flux closure and thus it is possibly related to tail reconnection which closes flux (Dungey-type). As the UVIS auroral observations do not allow us to estimate the open flux at the beginning of the sequence, we can not be certain on the origin of the event. However, from 2046 to 2253 UT and while the auroral dawn emission intensifies and grows spatially with time, one would expect ongoing closure of open flux for a Dungey-type reconnection driven event. Instead the open flux estimations (blue diamonds and red line on Figure 2) demonstrate that the amount of open flux remains almost constant (flux 2) or increases (flux 1) with time, depending on how one interprets the high-latitude feature. The shift of the main emission oval as described above (the afternoon sector shifts to lower latitudes while the pre-dawn region shifts poleward) which could be possibly attributed to the 1-2° dawn-dusk oscillations (Nichols et al., 2010) should not be confused with flux changes (closure or opening of flux). Given the estimated flux variations we suggest that the auroral dawn enhancement under study could be caused by internally driven reconnection, as the Dungey-type (solar wind driven) reconnection process would result in flux closure. It should be noted that opening of flux at the same rate as it closes would also result in the observed quasi-constant open flux. However, this possibility is less probable because, as mentioned before, this interval does not show auroral evidence of low-latitude reconnection which could justify opening of flux.

This event differs from a number of earlier studies in which auroral dawn enhancements are associated with tail reconnection, which closes open flux (Dungey-type tail reconnection) with rates between 200 kV and 1000 kV. Radioti et al. (2014) using the same method presented here, showed that intensifications in the dawn sector in a UVIS sequence are indicative of a flux closure rate which increases from 200 kV to 1000 kV within a couple of hours. During the last interval the open magnetic flux decreased from 34.5 to 31 GWb within $\sim$ 1 hour, corresponding to a reconnection rate of $\sim$1000 kV. Nichols et al. (2014) estimated a reconnection voltage of $\sim$ 280 kV corresponding to dawn enhancements during an HST sequence, based on the poleward propagation of the emission. Statistical analysis of HST auroral emissions were suggestive of tail reconnection flux closure rates ranging from a few tens of kV to 275 kV (Badman et al., 2014). The auroral enhancements in the dawn sector presented by Mitchell et al. (2009) did not include flux estimations and thus it was uncertain whether they were triggered by Dungey or Vasyliūnas type tail reconnection. Tail reconnection flux closure rates estimated based on magnetic field observations at Saturn range from 50 kV to 450 kV in strong solar wind compressions, while during short and active solar wind intervals this rate might be significantly higher (Jackman et al., 2004). Finally, based on observations of a post-plasmoid plasma sheet (Richardson et al., 1987) magnetic signature following plasmoid release at Saturn, it is estimated that 0.26-2.2 GWb of flux may be closed via tail reconnection over 27 minutes (Jackman et al., 2014).

Vasyliūnas type reconnection on closed field lines does not change the amount of open flux and the size of the polar cap. In the absence of Dungey type nightside reconnection, the Vasyliūnas reconnection x-line is expected to form primarily in the midnight to dawn sector (Jia et al., 2012; Cowley et al., 2005), consistent with present observations. However, the location of the auroral enhancement cannot be used as a determining criterion regarding the origin of the event but rather as supporting evidence, since the auroral signature of Dungey-type tail reconnection is also expected to be located in the same region (Cowley et al., 2005; Nichols et al., 2014; Radioti et al., 2014).

The rotation velocity of the enhanced region is observed to be 56% of rigid corotation in the beginning of the sequence and is observed to decrease with time up to 27% towards the end. The mean velocity is $\sim 45\%$ of rigid corotation, which is consistent with the predictions of MHD simulations (Jia et al., 2012) for auroral signatures of Vasyliūnas-type reconnection. The simulations suggest that, even though the details may vary from case to case depending on the state of the magnetosphere, the intensification of field-aligned currents in the ionosphere associated with Dungey reconnection rotates at an average rate close to or even above rigid corotation between post-midnight and noon sector, while for Vasyliūnas-type, the auroral feature typically rotates at $\sim 50\%$ rigid corotation on average, which is within the range of rotation rate in our observations. The difference in the outflow velocities between Vasyliūnas-type and Dungey-type reconnection is related to the Alfvén speed in the inflow region at the reconnection site. For Vasyliūnas-type reconnection, which involves mostly reconnection on closed plasma sheet field lines, the inflow Alfvén speed is generally smaller (of the order of 100 km/s). For Dungey-type (or solar wind driven) reconnection, field lines in the tail lobes also participate in the reconnection and thus Alfvén speed on those field lines is generally very high (of the order of 1000 km/s) because of the low densities in the lobes. Indeed, auroral enhancements related to Dungey-type tail reconnection are observed to rotate with higher velocities of $\sim$70% (Radioti et al., 2014) and in some cases Dungey-type auroral bursts (open-flux closure events) may reach extremely high velocities ($\sim 330\%$ rigid corotation) (Nichols et al., 2014).

Finally, the brightness of the dawn enhancement as mentioned above, displays features with a large range of brightness. Localised peaks could be as bright as 30 kR and others could reach values in excess of 300 kR. MHD simulations (Jia et al., 2012), suggest that Dungey-type reconnection typically results in hotter and more depleted flux tubes compared to those produced directly by the Vasyliūnas-type reconnection. The brightness values observed within this enhancement are inconclusive regarding the origin of the event.

The upper range of localised peaks observed here (> 100 kR) is of the same order of magnitude with events attributed to solar-wind driven tail reconnection (Nichols et al., 2014; Radioti et al., 2014), while the localised less bright features (< 100 kR) are consistent with internally driven reconnection events.

The auroral dawn enhancement reported here, given its observed location and brightness, is most probably due to hot tenuous plasma carried inward in fast moving flux tubes returning from a tail reconnection site to the dayside. These flux tubes could generate intense field-aligned currents that would cause aurora to brighten. However, whether this event is solar wind or internally driven is uncertain. Based on the flux variations, which do not demonstrate flux closure, we propose that the dawn enhancement is related to internally driven tail reconnection (Vasyliūnas-type) which operates on closed field lines. This is also supported by the location of the enhancement in the midnight-dawn quadrant (even though this alone can not prove the origin of the event as explained above) and the relative low rotational velocity of the event, which are both in accordance with the expectations of the auroral counterpart of Vasyliūnas-type tail reconnection events, according to MHD simulations (Jia et al., 2012).

3. Small scale structures within the large auroral enhancement

3.1. Dipolarization signatures, auroral vortices and streamers

During reconnection and associated dipolarization of the field, the inner edge of this tail current can be diverted through the ionosphere, in a situation analogous to the 'substorm current wedge' picture at Earth (McPherron et al., 1973). Close ups of the dawn enhancements shown in Figure 3, obtained from UVIS high-resolution images (panel a) indicate repetitive multiple intensifications on the main emission (image taken at 1942 UT) with spatial dimensions of $\sim 1.5°$ latitude $\times$ 5° longitude and brightness ranging from 20 to 40 kR. We magnetically map the auroral features on the equatorial plane using a current sheet model, considering a current sheet half thickness of 2.5 R_S, a magnetopause standoff distance of 22 and 27 R_S, consistent with Achilleos et al. (2008) inner and outer magnetopause boundary position, and the current sheet scaling laws from Bunce et al. (2007). Their location in the equatorail plane lies between 16 and 19 R_S and between 19 and 23 R_S for magnetopause boundary position 22 and 27 R_S, respectively. For the mapping we consider the latitudinal shift due to the aforementioned oscillations of the center of the main emission oval. These intensifications could be signatures of dipolarization and thus the onset of reconnection. This is consistent with previous studies (Jackman et al., 2013) which interpreted a similar spot-like intensification ($\sim 3°$ latitude $\times$ $9°$ longitude, maximum brightness of 16 - 35 kR, equatorial mapped location between $\sim$10 and 13 R_S) in the nightside sector as signature of dipolarization in the tail and the precursor to a more intense activity following tail reconnection. The reconnection x-line has been estimated to lie, on average, in the region of $\sim$20 to 30 R_S (Mitchell et al., 2005) based on Energetic Neutral Atom (ENA) emissions linked to reconnection events, which is somewhat further than our auroral intensifications. Also modelling work has suggested the position of the x-line to be highly sensitive to solar wind conditions and to vary from 25 to 40 R_S (Jia et al., 2012). In addition, a recent study (Jackman et al., 2014) suggested that the position of the x-line might be highly mobile, as there is no clear demarcation between the planetward and tailward events. Our observations are also indicative of multiple reconnection onsets along an extended x-line from $\sim$ 02 to 05 LT. We propose that tail reconnection at Saturn may take the form of multiple x-lines in the tail, by analogy with the Earth (Imber et al., 2011), even though in the terrestrial case it was suggested that the x-line is also extended in radial distance.

The observations reveal that soon after onset (images taken from 2046 UT to the end), the intensifications evolve with time into a series of spot- and arc-like structures. The arc-like structures observed at Saturn could be related to flows released from reconnection similar to the auroral streamers at Earth (i.e. Angelopoulos et al. (1996); Sergeev et al. (2004)). Auroral streamers have been related to enhanced earthward flows within the plasma sheet and to magnetic field dipolarizations, which connect to the ionosphere via field-aligned currents following the concept of a narrow current wedge (Birn et al., 2004). Similar auroral features have been related to inward moving flows released after tail reconnection at Jupiter (Radioti et al., 2010). If this is also the case at Saturn, then these observations would be suggestive of multiple narrow channels spread azimuthally and radially.

The small scale features occasionally resemble vortices, a picture that is especially evident in the image taken at 2149 UT in Figure 3. The formation of flow vorticity and associated FAC generation at Earth is predicted by several alternative scenarios related to substorms, such as plasma flow breaking (e.g., Shiokawa et al. (1997)) cross-field current instability (e.g., Lui et al. (1991)) and ballooning instabilities (e.g., Voronkov et al. (1997)). Auroral vortices surrounded by streamers have also been reported after substorm reconnection onset at Earth (Lyons et al., 2013), very similar to the observations shown here. Keiling et al. (2009), based on multi-spacecraft observations, suggested that space vortices generated the field-aligned current of the current wedge at the beginning of the substorm expansion phase and coupled to the ionosphere causing ionospheric vortices, according to the concept proposed by Birn et al. (2004).

Cassini plasma observations have shown evidence of numerous significant inflow events in the postmidnight sector following tail reconnection at Saturn (Thomsen et al., 2013). The large majority of the plasma flows are found to be within 20° of the corotation direction, though with flow speeds significantly lower than full corotation. Also fast (brief episodes of ∼10 minutes) planetward convective flows have been observed by the energetic particle detector onboard Cassini in the nightside magnetosphere (Mitchell et al., 2014a). They have been identified as transitional events between current sheet collapse and interchange. The brief periods of radial flow could set up vortical flow at their boundaries, assuming they are limited in azimuth. The simulations by Jia et al. (2012) predict fast plasma flows, released from tail reconnection at Saturn, to move towards the planet and create flow shear with the surroundings. Those rapidly moving flux tubes are expected to generate strong disturbances in the ionosphere. We suggest that the concept proposed by Birn et al. (2004) for the Earth might also be applicable to Saturn. Figure 3, panel b presents an illustration of the build up of field-aligned currents by vortex flow in the tail which could explain the formation of auroral vortices and streamers during dipolarization current wedge (adapted from Birn et al. (2004)). According to this model, planetward moving flow pushes the neighbouring field lines and causes a twist or shear in the magnetic field.

Finally, our results indicate that the evolution of tail reconnection at Saturn may not be pictured with a single current wedge. Instead the multiple intensifications and streamers indicate that the evolution of tail reconnection can be explained by an ensemble of many narrow current wedges or that inward transport related to the reconnection region could be explained by multiple localised flow burst events in analogy to the terrestrial case (e.g. Nakamura et al. (1994); Lyons et al. (2013)).

3.2. *Auroral signatures of viscous interaction of the solar wind with the magnetosphere*

Alternatively to the aforementioned interpretation, one could suggest that the dawn small scale features observed here are auroral signatures of viscous interaction of the solar wind with the magnetosphere. Delamere and Bagenal (2013) proposed that viscous interaction involves magnetic reconnection on a small scale, thus facilitating intermittent reconnection. Cassini observations of a plasma vortex in Saturn's dayside outer magnetosphere were suggestive of the presence of nonlinear Kelvin-Helmholtz instability at Saturn's morning magnetospheric boundaries (Masters et al., 2010). However, recent global survey based on Cassini data from 2004 to 2009 revealed that most of the potential Kelvin-Helmholtz activity is on the dusk flank (Delamere et al., 2013). Masters et al. (2010) proposed that plasma vortices related to Kelvin-Helmholtz instability could result in the formation of field-aligned current systems which could give rise to vortex footprints in the ionosphere. Small scale structures on the main UV emission located at noon and in dusk sector have been previously reported (Grodent et al., 2011) and are related to patterns of upward field-aligned currents resulting from non-uniform plasma flow in the equatorial plane possibly triggered by magnetopause Kelvin-Helmholtz waves. These auroral features had brightness up to 30 kR and were not part of a major auroral enhancement, while the observations here are indicative of much brighter small scale features (up to 300 kR). Additionally, the observed emissions are confined to the dawn sector while most of the potential Kelvin-Helmholtz activity is on the dusk flank according to Delamere et al. (2013). Therefore we suggest that it is less plausible that the present observations bear a signature of viscous interaction involving magnetic reconnection on small scale such as proposed by Delamere and Bagenal (2013).

4. Summary and conclusions

We present high-resolution UVIS observations of Saturn's aurora during the DOY 140-141, 2013. The observations reveal an enhanced activity in the midnight-dawn quadrant. The region extends from ~02 to 05 LT and propagates with time up to 10 LT. It has an average brightness of ~ 150 kR, while it rotates with an average velocity of ~45% of rigid corotation. The morphology of the feature is consistent with the auroral signatures of bursts of tail reconnection discussed in earlier theoretical and observational studies (Cowley et al., 2005; Mitchell et al., 2009; Clarke et al., 2009; Jia et al., 2012; Nichols et al., 2014; Radioti et al., 2014). Given its observed location and brightness, it is most probably due to hot tenuous plasma carried inward in fast moving flux tubes returning from tail reconnection site to the dayside. These flux tubes could generate intense field-aligned currents that would cause aurora to brighten. Whether this event is attributed to solar wind (Dungey-type) or internally driven (Vasyliūnas-type) reconnection is uncertain. However, based on the open flux variations during this sequence (red line on Figure 2), which do not demonstrate flux closure, the event is possibly indicative of Vasyliūnas type reconnection on closed field lines which does not modify the amount of open flux. In the absence of Dungey type nightside reconnection, which could be the case for a period of southward IMF, the Vasyliūnas reconnection x-line is expected to form primarily in the midnight to dawn sector (Jia et al., 2012; Cowley et al., 2005) in accordance with our observations. Additionally, the rotation velocity of the enhanced region is observed to be on average $\sim 45\%$ of rigid corotation, which is consistent with the predictions of MHD simulations (Jia et al., 2012) for auroral signatures of Vasyliūnas-type reconnection. The auroral signature associated with Dungey type reconnection rotates at much larger average rates close to or even above rigid corotation. It should be noted, however, that the brightness of the dawn enhancement is inconclusive regarding the origin of the event, since the enhancement region exhibits localised peaks with a large range of brightness, which could be attributed to both types of tail reconnection.

Our observations also reveal multiple intensifications indicative of an x-line in the tail which extends from 02 to 05 LT. The localised enhancements evolve in arc and spot-like features, which resemble vortices mainly in the beginning of the sequence. These features could be related to flows released from reconnection that are separated into multiple narrow channels spread azimuthally and radially. We suggest that the evolution of tail reconnection at Saturn may not be pictured by a single current wedge. Instead the multiple intensifications and substructures indicate that the evolution of tail reconnection can be explained by an ensemble of many narrow current wedges or that inward transport related to the reconnection region could be explained by multiple localised flow bursts events similar to the picture proposed for Earth (Nakamura et al., 1994; Lyons et al., 2013). Although the reason for the formation of vortical-like structures remains unknown, one possibility could be that they are attributed to field-aligned currents, which are build up by vortex flow in the tail (Birn et al., 2004). A less plausible scenario could be that the small scale structures are related to viscous interactions involving small-scale reconnection.

acknowledgments

This work is based on observations with the UVIS instrument onboard the NASA/ESA Cassini spacecraft. The research was supported by (F.R.S. - FNRS) and the PRODEX Program managed by the European Space Agency in collaboration with the Belgian Federal Science Policy Office. B.B. is funded by FNRS. X.J. acknowledges the support by NASA through grant NNX12AK34G and by the Cassini mission under contract JPL 1409449. CMJ's work at Southampton is supported by a Science and Technology Facilities Council Ernest Rutherford Fellowship. A.R. gratefully acknowledges Gabrielle Provan for providing the azimuthal directions of the effective dipoles.

References

Achilleos, N., Arridge, C.S., Bertucci, C., Jackman, C.M., Dougherty, M.K., Khurana, K.K., Russell, C.T., 2008. Large-scale dynamics of Saturn's magnetopause: Observations by Cassini. Journal of Geophysical Research (Space Physics) 113, 11209.

Angelopoulos, V., Coroniti, F.V., Kennel, C.F., Kivelson, M.G., Walker, R.J., Russell, C.T., McPherron, R.L., Sanchez, E., Meng, C.I., Baumjohann, W., Reeves, G.D., Belian, R.D., Sato, N., Friis-Christensen, E., Sutcliffe, P.R., et al., 1996. Multipoint analysis of a bursty bulk flow event on April 11, 1985. Journal of Geophysical Research 101, 4966–4990.

Badman, S.V., Andrews, D.J., Cowley, S.W.H., Lamy, L., Provan, G., Tao, C., Kasahara, S., Kimura, T., Fujimoto, M., Melin, H., Stallard, T., Brown, R.H., Baines, K.H., 2012. Rotational modulation and local time dependence of Saturn's infrared H_3^+ auroral intensity. Journal of Geophysical Research (Space Physics) 117, 9228.

Badman, S.V., Bunce, E.J., Clarke, J.T., Cowley, S.W.H., GéRard, J.C., Grodent, D., Milan, S.E., 2005. Open flux estimates in Saturn's magnetosphere during the January 2004 Cassini-HST campaign, and implications for reconnection rates. Journal of Geophysical Research (Space Physics) 110, 11216.

Badman, S.V., Cowley, S.W.H., 2007. Significance of Dungey-cycle flows in Jupiter's and Saturn's magnetospheres, and their identification on closed equatorial field lines. Annales Geophysicae 25, 941–951.

Badman, S.V., Jackman, C.M., Nichols, J.D., Clarke, J.T., Gérard, J.C., 2014. Open flux in Saturn's magnetosphere. Icarus 231, 137–145.

Birn, J., Raeder, J., Wang, Y., Wolf, R., Hesse, M., 2004. On the propagation of bubbles in the geomagnetic tail. Annales Geophysicae 22, 1773–1786.

Bunce, E.J., Arridge, C.S., Clarke, J.T., Coates, A.J., Cowley, S.W.H., Dougherty, M.K., GéRard, J.C., Grodent, D., Hansen, K.C., Nichols, J.D., Southwood, D.J., Talboys, D.L., 2008. Origin of Saturn's aurora: Simultaneous observations by Cassini and the Hubble Space Telescope. Journal of Geophysical Research (Space Physics) 113, 9209.

Bunce, E.J., Cowley, S.W.H., Alexeev, I.I., Arridge, C.S., Dougherty, M.K., Nichols, J.D., Russell, C.T., 2007. Cassini observations of the variation of Saturn's ring current parameters with system size. Journal of Geophysical Research (Space Physics) 112, 10202.

Bunce, E.J., Cowley, S.W.H., Yeoman, T.K., 2004. Jovian cusp processes: Implications for the polar aurora. Journal of Geophysical Research (Space Physics) 109, 9.

Clarke, J.T., Nichols, J., Gérard, J.C., Grodent, D., Hansen, K.C., Kurth, W., Gladstone, G.R., Duval, J., Wannawichian, S., Bunce, E., Cowley, S.W.H., Crary, F., Dougherty, M., Lamy, L., Mitchell, D., Pryor, W., Retherford, K., Stallard, T., Zieger, B., Zarka, P., Cecconi, B., 2009. Response of Jupiter's and Saturn's auroral activity to the solar wind. Journal of Geophysical Research (Space Physics) 114, 5210.

Cowley, S.W.H., Badman, S.V., Bunce, E.J., Clarke, J.T., GéRard, J.C., Grodent, D., Jackman, C.M., Milan, S.E., Yeoman, T.K., 2005. Reconnection in a rotation-dominated magnetosphere and its relation to Saturn's auroral dynamics. Journal of Geophysical Research (Space Physics) 110, 2201.

Delamere, P.A., Bagenal, F., 2013. Magnetotail structure of the giant magnetospheres: Implications of the viscous interaction with the solar wind. Journal of Geophysical Research (Space Physics) 118, 7045–7053.

Delamere, P.A., Wilson, R.J., Eriksson, S., Bagenal, F., 2013. Magnetic signatures of Kelvin-Helmholtz vortices on Saturn's magnetopause: Global survey. Journal of Geophysical Research (Space Physics) 118, 393–404.

Dungey, J.W., 1961. Interplanetary magnetic field and the auroral zones. Physical Review Letters .

Esposito, L.W., Barth, C.A., Colwell, J.E., Lawrence, G.M., McClintock, W.E., Stewart, A.I.F., Keller, H.U., Korth, A., Lauche, H., Festou, M.C., Lane, A.L., Hansen, C.J., Maki, J.N., West, R.A., Jahn, H., Reulke, R., Warlich, K., Shemansky, D.E., Yung, Y.L., 2004. The Cassini Ultraviolet Imaging Spectrograph Investigation. Space Science Review 115, 299–361.

Gérard, J.C., Bunce, E.J., Grodent, D., Cowley, S.W.H., Clarke, J.T., Badman, S.V., 2005. Signature of Saturn's auroral cusp: Simultaneous Hubble Space Telescope FUV observations and upstream solar wind monitoring. Journal of Geophysical Research (Space Physics) 110, 11201.

Grodent, D., Gustin, J., Gérard, J.C., Radioti, A., Bonfond, B., Pryor, W.R., 2011. Small-scale structures in Saturn's ultraviolet aurora. Journal of Geophysical Research (Space Physics) 116, 9225.

Imber, S.M., Slavin, J.A., Auster, H.U., Angelopoulos, V., 2011. A THEMIS survey of flux ropes and traveling compression regions: Location of the near-Earth reconnection site during solar minimum. Journal of Geophysical Research (Space Physics) 116, 2201.

Jackman, C.M., Achilleos, N., Bunce, E.J., Cowley, S.W.H., Dougherty, M.K., Jones, G.H., Milan, S.E., Smith, E.J., 2004. Interplanetary magnetic field at 9 AU during the declining phase of the solar cycle and its implications for Saturn's magnetospheric dynamics. Journal of Geophysical Research (Space Physics) 109, 11203.

Jackman, C.M., Achilleos, N., Cowley, S.W.H., Bunce, E.J., Radioti, A., Grodent, D., Badman, S.V., Dougherty, M.K., Pryor, W., 2013. Auroral counterpart of magnetic field dipolarizations in Saturn's tail. Planetary and Space Science 82, 34–42.

Jackman, C.M., Cowley, S.W.H., 2006. A model of the plasma flow and current in Saturn's polar ionosphere under conditions of strong Dungey cycle driving. Annales Geophysicae 24, 1029–1055.

Jackman, C.M., Slavin, J.A., Cowley, S.W.H., 2011. Cassini observations of plasmoid structure and dynamics: Implications for the role of magnetic reconnection in magnetospheric circulation at Saturn. Journal of Geophysical Research (Space Physics) 116, 10212.

Jackman, C.M., Slavin, J.A., Kivelson, M.G., Southwood, D.J., Achilleos, N., Thomsen, M.F., DiBraccio, G.A., Eastwood, J.P., Freeman, M.P., Dougherty, M.K., Vogt, M.F., 2014. Saturn's dynamic magnetotail: A comprehensive magnetic field and plasma survey of plasmoids and traveling compression regions and their role in global magnetospheric dynamics. Journal of Geophysical Research (Space Physics) 119, 5465–5494.

Jia, X., Hansen, K.C., Gombosi, T.I., Kivelson, M.G., Tóth, G., DeZeeuw, D.L., Ridley, A.J., 2012. Magnetospheric configuration and dynamics of Saturn's magnetosphere: A global MHD simulation. Journal of Geophysical Research (Space Physics) 117, 5225.

Keiling, A., Angelopoulos, V., Runov, A., Weygand, J., Apatenkov, S.V., Mende, S., McFadden, J., Larson, D., Amm, O., Glassmeier, K.H., Auster, H.U., 2009. Substorm current wedge driven by plasma flow vortices: THEMIS observations. Journal of Geophysical Research (Space Physics) 114, 0.

Lui, A.T.Y., Chang, C.L., Mankofsky, A., Wong, H.K., Winske, D., 1991. A cross-field current instability for substorm expansions. Journal of Geophysical Research 96, 11389.

Lyons, L.R., Nishimura, Y., Donovan, E., Angelopoulos, V., 2013. Distinction between auroral substorm onset and traditional ground magnetic onset signatures. Journal of Geophysical Research (Space Physics) 118, 4080–4092.

Masters, A., Achilleos, N., Kivelson, M.G., Sergis, N., Dougherty, M.K., Thomsen, M.F., Arridge, C.S., Krimigis, S.M., McAndrews, H.J., Kanani, S.J., Krupp, N., Coates, A.J., 2010. Cassini observations of a Kelvin-Helmholtz vortex in Saturn's outer magnetosphere. Journal of Geophysical Research (Space Physics) 115, 7225.

McPherron, R.L., Russell, C.T., Aubry, M.P., 1973. Satellite studies of magnetospheric substorms on August 15, 1968: 9. Phenomenological model for substorms. Journal of Geophysical Research 78, 3131.

Mitchell, D.G., Brandt, P.C., Carbary, J.F., Kurth, W.S., Krimigis, S.M., Paranicas, C., Krupp, N., Hamilton, D.C., Mauk, B.H., Hospodarsky, G.B., Dougherty, M.K., Pryor, W.R., 2014a. Injection, Interchange, and Reconnection: Energetic Particle Observations in Saturns Magnetosphere. Magnetotail in the Solar System, Geophysical Monograph .

Mitchell, D.G., Brandt, P.C., Roelof, E.C., Dandouras, J., Krimigis, S.M., Mauk, B.H., Paranicas, C.P., Krupp, N., Hamilton, D.C., Kurth, W.S., Zarka, P., Dougherty, M.K., Bunce, E.J., Shemansky, D.E., 2005. Energetic ion acceleration in Saturn's magnetotail: Substorms at Saturn? Geophysical Research Letters 32, 20.

Mitchell, D.G., Carbary, J.F., Bunce, E.J., Radioti, A., Badman, S.V., Pryor, W.R., Hospodarsky, G.B., Kurth, W.S., 2014b. Recurrent Pulsations in Saturns High Latitude Magnetosphere. Icarus .

Mitchell, D.G., Krimigis, S.M., Paranicas, C., Brandt, P.C., Carbary, J.F., Roelof, E.C., Kurth, W.S., Gurnett, D.A., Clarke, J.T., Nichols, J.D., Gérard, J.C., Grodent, D.C., Dougherty, M.K., Pryor, W.R., 2009. Recurrent energization of plasma in the midnight-to-dawn quadrant of Saturn's magnetosphere, and its relationship to auroral UV and radio emissions. Planetary and Space Science 57, 1732–1742.

Nakamura, R., Baker, D.N., Yamamoto, T., Belian, R.D., Bering, III, E.A., Benbrook, J.R., Theall, J.R., 1994. Particle and field signatures during pseudobreakup and major expansion onset. Journal of Geophysical Research 99, 207–221.

Nichols, J.D., Badman, S.V., Baines, K.H., Brown, R.H., Bunce, E.J., Clarke, J.T., Cowley, S.W.H., Crary, F.J., Dougherty, M.K., Gérard, J.C., Grocott, A., Grodent, D., Kurth, W.S., Melin, H., Mitchell, D.G., Pryor, W.R., Stallard, T.S., 2014. Dynamic auroral storms on Saturn as observed by the Hubble Space Telescope. Geophysical Research Letters 41, 3323–3330.

Nichols, J.D., Cowley, S.W.H., Lamy, L., 2010. Dawn-dusk oscillation of Saturn's conjugate auroral ovals. Geophysical Research Letters 37, 24102.

Provan, G., Cowley, S.W.H., Sandhu, J., Andrews, D.J., Dougherty, M.K., 2013. Planetary period magnetic field oscillations in Saturn's magnetosphere: Postequinox abrupt nonmonotonic transitions to northern system dominance. Journal of Geophysical Research (Space Physics) 118, 3243–3264.

Pryor, W. R., e.a., 2012. Ultraviolet auroral pulsations on Saturn from Cassini UVIS, in: DPS 44, Reno, Nevada, Bull. American Astronomical Soc., 44, 5, presentation 413.05.

Radioti, A., Grodent, D., Gérard, J.C., Bonfond, B., 2010. Auroral signatures of flow bursts released during magnetotail reconnection at Jupiter. Journal of Geophysical Research (Space Physics) 115, 7214.

Radioti, A., Grodent, D., Gérard, J.C., Milan, S.E., Bonfond, B., Gustin, J., Pryor, W., 2011. Bifurcations of the main auroral ring at Saturn: ionospheric signatures of consecutive reconnection events at the magnetopause. Journal of Geophysical Research (Space Physics) 116, 11209.

Radioti, A., Grodent, D., Gérard, J.C., Milan, S.E., Fear, R.C., Jackman, C.M., Bonfond, B., Pryor, W., 2014. Saturn's elusive nightside polar arc. Geophysical Research Letters .

Richardson, I.G., Cowley, S.W.H., Hones, Jr., E.W., Bame, S.J., 1987. Plasmoid-associated energetic ion bursts in the deep geomagnetic tail - Properties of plasmoids and the postplasmoid plasma sheet. Journal of Geophysical Research 92, 9997–10013.

Sergeev, V., Liou, K., Newell, P., Ohtani, S., Hairston, M., Rich, F., 2004. Auroral streamers: characteristics of associated precipitation,convection and field-aligned currents. Annales Geophysicae 22, 537–548.

Shiokawa, K., Baumjohann, W., Haerendel, G., 1997. Braking of high-speed flows in the near-Earth tail. Geophysical Research Letters 24, 1179–1182.

Thomsen, M.F., Wilson, R.J., Tokar, R.L., Reisenfeld, D.B., Jackman, C.M., 2013. Cassini/CAPS observations of duskside tail dynamics at Saturn. Journal of Geophysical Research (Space Physics) 118, 5767–5781.

Vasyliūnas, V.M., 1983. Plasma distribution and flow. Physics of the Jovian Magnetosphere, Cambridge Univ. Press.

Voronkov, I., Rankin, R., Frycz, P., Tikhonchuk, V.T., Samson, J.C., 1997. Coupling of shear flow and pressure gradient instabilities. Journal of Geophysical Research 102, 9639–9650.

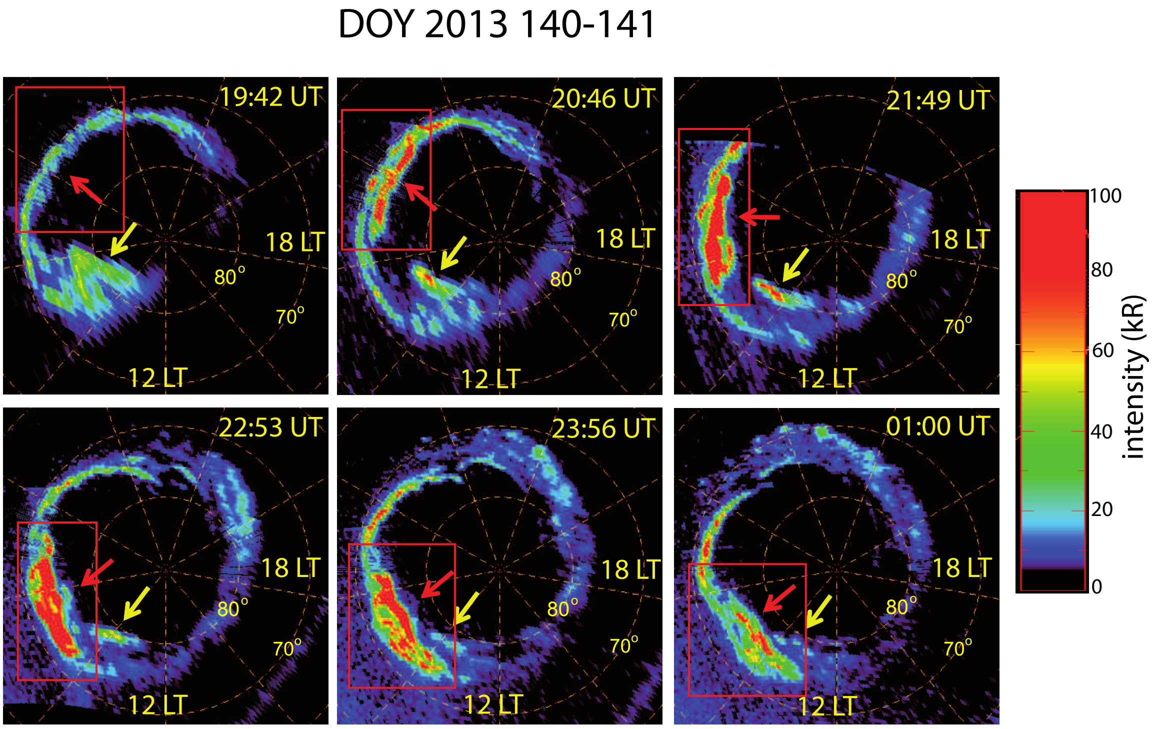

Figure 1: A sequence of polar projections of Saturn's northern aurora obtained with the FUV channel of UVIS onboard Cassini. The first image starts at 1942 UT on DOY 140, 2013 and the last one at 0100 UT on DOY 141, 2013. Noon is to the bottom and dusk to the right. The grid shows latitudes at intervals of 10° and meridians of 40°. The red rectangles include the auroral intensifications in the dawn-midnight quadrant, related to bursts of tail reconnection. Yellow arrows point to an auroral feature that was left over from a previous reconnection event. The color scale is saturated to 100 kR, as shown in the color bar to the right. The polar projection procedure does not preserve photometry; therefore, the colour table may only be used as a proxy for the projected emission brightness.

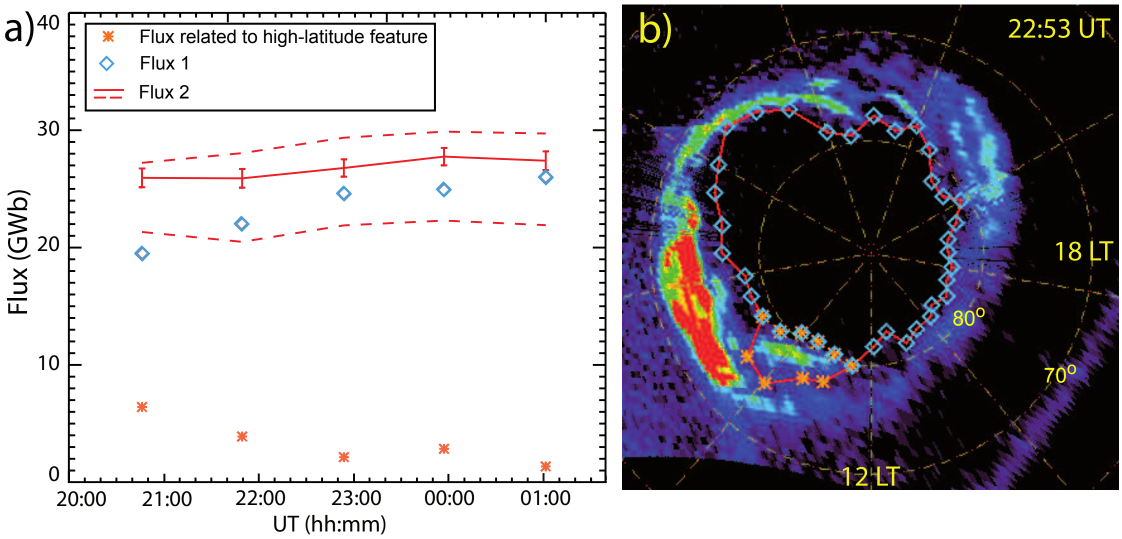

Figure 2: Panel a: Flux variations as a function of time, based on the observed auroral sequence in Figure 1. The polar cap boundaries are estimated automatically based on the cut-off intensity (4 kR), which corresponds to an average value of the day and night glow emission of these observations. The orange asterisks stand for the flux of the high latitude emission pointed out by the yellow arrow in Figure 1, which could be related either to high latitude reconnection (open flux) or excess flux of the bursty reconnection of lobe flux (closed flux). The blue diamonds correspond to 'flux 1', which is the total open flux at a given time assuming that the high latitude feature is related to closed flux. The red line corresponds to 'flux 2', which is the total open flux at a given time considering that the high latitude feature is related to open flux. Red dashed lines correspond to 'flux 2' estimated for the extreme thresholds of 3 kR (bottom line) and 5 kR (top line). The error bars indicate the statistical error related to the number of counts included in our initial chosen threshold of 4 kR. Panel b: A polar projection of Saturn's aurora taken at 2253 UT during the sequence shown in Figure 1. The different symbols draw the boundaries used to derive the different types of flux variations.

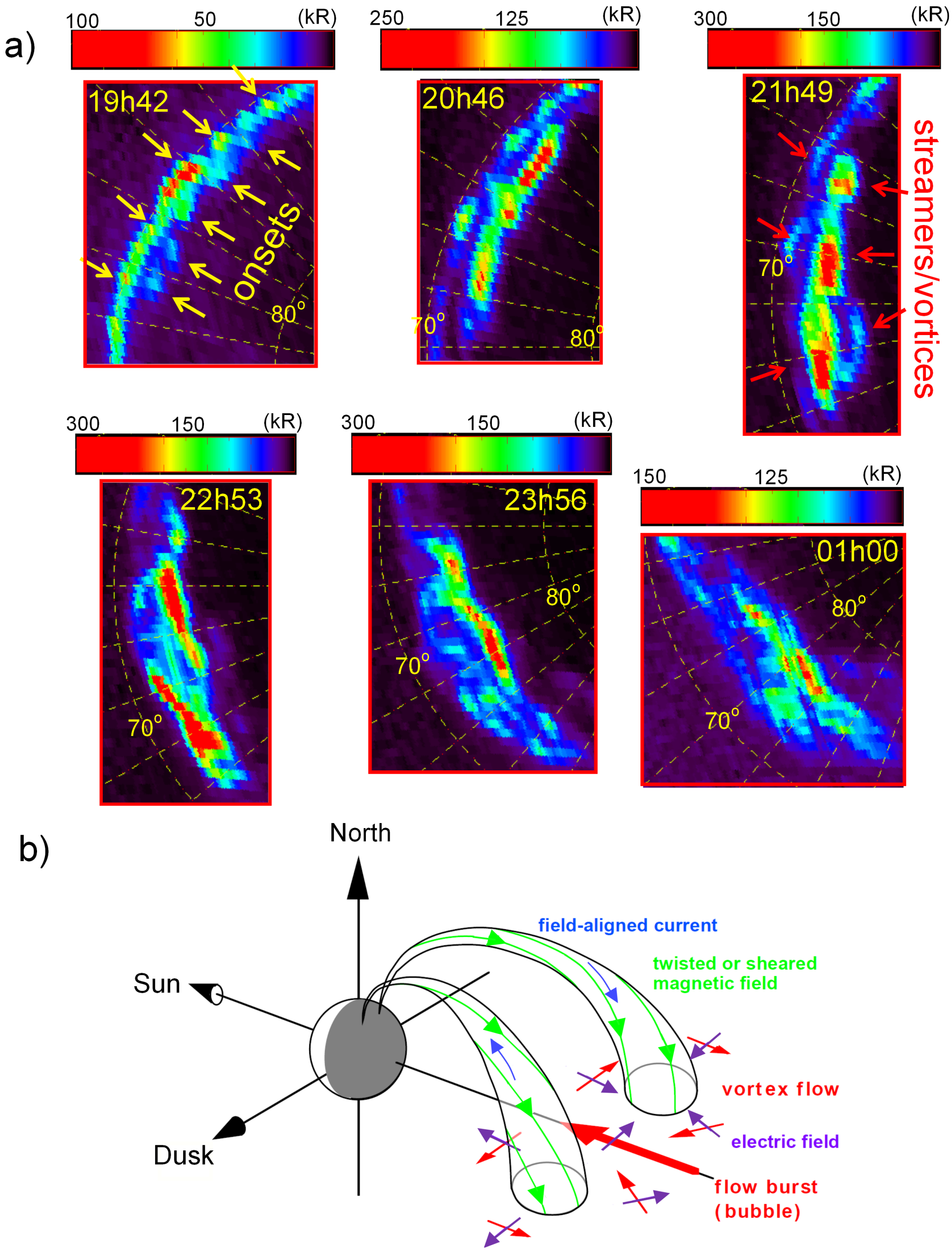

Figure 3: Panel a: Projected close-ups of a selected auroral region, indicated with the red rectangles on the complete projections of Figure 1. A single subimage is used for the close ups. The grid shows meridians of 10° and the latitudes are indicated. Yellow arrows indicate intensifications, which are discussed in the text as reconnection onsets. Red arrows indicate arc- and spot-like structures, which are discussed in the text as streamers and vortices. In order to highlight the details of the auroral structure the colorscale used is different for each panel. The polar projection procedure does not preserve photometry; therefore, the colour table may only be used as a proxy for the projected emission brightness. Panel b: Schematic illustrating the build-up of field-aligned currents by vortex flow in the tail adapted for Saturn from the terrestrial case (Birn et al., 2004).